

of a threshold difference for the therapeutic and side effects of RXR agonists. We believe that RXR partial agonists such as **11b** represent a promising class of candidate antitype 2 diabetes agents.

■ ASSOCIATED CONTENT

Supporting Information

General information, synthetic procedures, combustion analysis data, HPLC charts, luciferase reporter gene assay, and in vivo experimental procedures. This material is available free of charge via the Internet at <http://pubs.acs.org>.

■ AUTHOR INFORMATION

Corresponding Author

*Tel & Fax: +81-(0)86-251-7963. E-mail: kakuta@pharm.okayama-u.ac.jp.

Author Contributions

H.K. conceived and designed the project. N.Y., R.S., and M.H. synthesized compounds. F.O., S.Y., and Y.O. performed reporter gene assays. M.M. prepared plasmids. K.K., M.N., and C.F. performed in vivo experiments with ICR mice and SD rats. A.T. performed HPLC analysis. Y.Y. and H.Y. performed in vivo experiments with KK-A^y mice. C.F., S.U., A.M., M.N., and T.O. performed PCR analysis. The manuscript was written by H.K. and F.O.

Funding

This work was supported by Health and Labour Science research grants for Research on seeds for Publicly Essential Drugs and Medical Devices (23080401) from the Ministry of Health, Labour, and Welfare of Japan. We also thank the Ministry of Education, Science, Culture and Sports of Japan, and Takeda Science Foundation for financial support.

Notes

The authors declare no competing financial interest.

■ ACKNOWLEDGMENTS

We thank Dr. Miyachi (Okayama University) for kindly providing TIPP703 and carba-T0901317. We also thank Dr. Kagechika (School of Biomedical Science, Tokyo Medical and Dental University) for kindly providing PA452. The authors are also grateful to Professor Yoshio Naomoto and Dr. Takuya Fukazawa (Department of General Surgery, Kawasaki Medical School) for preparing plasmids. We also thank Dr. Aiba (Okayama University) for assistance with dissection.

■ ABBREVIATIONS

RXR, retinoid X receptor; PPAR, peroxisome proliferator-activated receptors; LXR, liver X receptor; RAR, retinoic acid receptor; TG, triglyceride; RT-PCR, reverse transcriptase polymerase chain reaction; *Irs*, insulin receptor substrate; GLUT, glucose transporter; *G6p*, glucose-6-phosphatase; *Pck*, phosphoenolpyruvate carboxykinase; *Gck*, glucokinase; *Scd1*, stearoyl-CoA desaturase 1; *Fasn*, fatty acid synthase; *Srebp1c*, sterol regulatory element-binding protein 1c

■ REFERENCES

(1) Kanda, S.; Nakashima, R.; Takahashi, K.; Tanaka, J.; Ogawa, J.; Ogata, T.; Yachi, M.; Araki, K.; Ohsumi, J. Potent antidiabetic effects of rivoglitazone, a novel peroxisome proliferator-activated receptor- γ agonist, in obese diabetic rodent models. *J. Pharmacol. Sci.* **2009**, *111*, 155–166.

(2) Mitro, N.; Mak, P. A.; Vargas, L.; Godio, C.; Hampton, E.; Molteni, V.; Kreusch, A.; Saez, E. The nuclear receptor LXR is a glucose sensor. *Nature* **2007**, *445*, 219–213.

(3) Svensson, S.; Ostberg, T.; Jacobsson, M.; Norström, C.; Stefansson, K.; Hallén, D.; Johansson, I. C.; Zachrisson, K.; Ogg, D.; Jendeborg, L. Crystal structure of the heterodimeric complex of LXR α and RXR β ligand-binding domains in a fully agonistic conformation. *EMBO J.* **2003**, *22*, 4625–4633.

(4) de Lera, A. R.; Bourguet, W.; Altucci, L.; Gronemeyer, H. Design of selective nuclear receptor modulators: RAR and RXR as a case study. *Nat. Rev. Drug Discovery* **2007**, *6*, 811–820.

(5) Mangelsdorf, D. J.; Evans, R. M. The RXR heterodimers and orphan receptors. *Cell* **1995**, *83*, 841–850.

(6) Laffitte, B. A.; Chao, L. C.; Li, J.; Walczak, R.; Hummasti, S.; Joseph, S. B.; Castrillo, A.; Wilpitz, D. C.; Mangelsdorf, D. J.; Collins, J. L.; Saez, E.; Tontonoz, P. Activation of liver X receptor improves glucose tolerance through coordinate regulation of glucose metabolism in liver and adipose tissue. *Proc. Natl. Acad. Sci. U.S.A.* **2003**, *100*, 5419–5424.

(7) Ogihara, T.; Chuang, J. C.; Vestermark, G. L.; Garmey, J. C.; Ketchum, R. J.; Huang, X.; Brayman, K. L.; Thorner, M. O.; Repa, J. J.; Mirmira, R. G.; Evans-Molina, C. Liver X receptor agonists augment human islet function through activation of anaplerotic pathways and glycerolipid/free fatty acid cycling. *J. Biol. Chem.* **2010**, *285*, 5392–5404.

(8) Shulman, A. I.; Larson, C.; Mangelsdorf, D. J.; Ranganathan, R. Structural determinants of allosteric ligand activation in RXR heterodimers. *Cell* **2004**, *116*, 417–429.

(9) Mukherjee, R.; Davies, P. J.; Crombie, D. L.; Bischoff, E. D.; Cesario, R. M.; Jow, L.; Hamann, L. G.; Boehm, M. F.; Mondon, C. E.; Nadzan, A. M.; Paterniti, J. R., Jr.; Heyman, R. A. Sensitization of diabetic and obese mice to insulin by retinoid X receptor agonists. *Nature* **1997**, *386*, 407–410.

(10) Davies, P. J.; Berry, S. A.; Shipley, G. L.; Eckel, R. H.; Hennuyer, N.; Crombie, D. L.; Ogilvie, K. M.; Peinado-Onsurbe, J.; Fievet, C.; Leibowitz, M. D.; Heyman, R. A.; Auwerx, J. Metabolic effects of rexinoids: tissue-specific regulation of lipoprotein lipase activity. *Mol. Pharmacol.* **2001**, *59*, 170–176.

(11) Li, X.; Hansen, P. A.; Xi, L.; Chandraratna, R. A.; Burant, C. F. Distinct mechanisms of glucose lowering by specific agonists for peroxisomal proliferator activated receptor γ and retinoic acid X receptors. *J. Biol. Chem.* **2005**, *280*, 38317–38327.

(12) Lenhard, J. M.; Lancaster, M. E.; Paulik, M. A.; Weiel, J. E.; Binz, J. G.; Sundseth, S. S.; Gaskill, B. A.; Lightfoot, R. M.; Brown, H. R. The RXR agonist LG100268 causes hepatomegaly, improves glycaemic control and decreases cardiovascular risk and cachexia in diabetic mice suffering from pancreatic beta-cell dysfunction. *Diabetologia* **1999**, *42*, 545–554.

(13) Liu, S.; Ogilvie, K. M.; Klausning, K.; Lawson, M. A.; Jolley, D.; Li, D.; Bilakovics, J.; Pascual, B.; Hein, N.; Urcan, M.; Leibowitz, M. D. Mechanism of selective retinoid X receptor agonist-induced hypothyroidism in the rat. *Endocrinology* **2002**, *143*, 2880–2885.

(14) Nishimaki-Mogami, T.; Tamehiro, N.; Sato, Y.; Okuhira, K.; Sai, K.; Kagechika, H.; Shudo, K.; Abe-Dohmae, S.; Yokoyama, S.; Ohno, Y.; Inoue, K.; Sawada, J. The RXR agonists PA024 and HX630 have different abilities to activate LXR/RXR and to induce ABCA1 expression in macrophage cell lines. *Biochem. Pharmacol.* **2008**, *76*, 1006–1013.

(15) Fujii, S.; Ohsawa, F.; Yamada, S.; Shinozaki, R.; Fukai, R.; Makishima, M.; Enomoto, S.; Tai, A.; Kakuta, H. Modification at the acidic domain of RXR agonists has little effect on permissive RXR-heterodimer activation. *Bioorg. Med. Chem. Lett.* **2010**, *20*, 5139–5142.

(16) Takamatsu, K.; Takano, A.; Yakushiji, N.; Morohashi, K.; Morishita, K.; Matsuura, N.; Makishima, M.; Tai, A.; Sasaki, K.; Kakuta, H. The first potent subtype-selective retinoid X receptor (RXR) agonist possessing a 3-isopropoxy-4-isopropylphenylamino moiety, NEt-3IP (RXR α / β -dual agonist). *ChemMedChem* **2008**, *3*, 780–787.

(17) Ohsawa, F.; Morishita, K.; Yamada, S.; Makishima, M.; Kakuta, H. Modification at the Lipophilic Domain of RXR Agonists Differentially Influences Activation of RXR Heterodimers. *ACS Med. Chem. Lett.* **2010**, *1*, 521–525.

(18) Kakuta, H.; Ohsawa, F.; Yamada, S.; Makishima, M.; Tai, A.; Yasui, H.; Yoshikawa, Y. Feasibility of Structural Modification of Retinoid X Receptor Agonists to Separate Blood Glucose-Lowering Action from Adverse Effects: Studies in KK-*A^y* Type 2 Diabetes Model Mice. *Biol. Pharm. Bull.* **2012**, *35*, 629–633.

(19) Yamauchi, T.; Waki, H.; Kamon, J.; Murakami, K.; Motojima, K.; Komeda, K.; Miki, H.; Kubota, N.; Terauchi, Y.; Tsuchida, A.; Tsuboyama-Kasaoka, N.; Yamauchi, N.; Ide, T.; Hori, W.; Kato, S.; Fukayama, M.; Akanuma, Y.; Ezaki, O.; Itai, A.; Nagai, R.; Kimura, S.; Tobe, K.; Kagechika, H.; Shudo, K.; Kadowaki, T. Inhibition of RXR and PPAR γ ameliorates diet-induced obesity and type 2 diabetes. *J. Clin. Invest.* **2001**, *108*, 1001–1013.

(20) Zhang, H.; Zhou, R.; Li, L.; Chen, J.; Chen, L.; Li, C.; Ding, H.; Yu, L.; Hu, L.; Jiang, H.; Shen, X. Danthron functions as a retinoic X receptor antagonist by stabilizing tetramers of the receptor. *J. Biol. Chem.* **2011**, *286*, 1868–1875.

(21) Kasuga, J.; Oyama, T.; Hirakawa, Y.; Makishima, M.; Morikawa, K.; Hashimoto, Y.; Miyachi, H. Improvement of the transactivation activity of phenylpropanoic acid-type peroxisome proliferator-activated receptor pan agonists: effect of introduction of fluorine at the linker part. *Bioorg. Med. Chem. Lett.* **2008**, *18*, 4525–8.

(22) Aoyama, A.; Aoyama, H.; Dodo, K.; Makishima, M.; Hashimoto, Y.; Miyachi, H. LXR antagonists with a 5-substituted phenanthridin-6-one skeleton: synthesis and LXR transrepression activities of conformationally restricted carba-T0901317 analogs. *Heterocycles* **2008**, *76*, 137–142.

(23) Heim, M.; Johnson, J.; Boess, F.; Bendik, I.; Weber, P.; Hunziker, W.; Fluhmann, B. Phytanic acid, a natural peroxisome proliferator-activated receptor (PPAR) agonist, regulates glucose metabolism in rat primary hepatocytes. *FASEB J.* **2002**, *16*, 718–720.

(24) Kim, S. Y.; Kim, H. I.; Kim, T. H.; Im, S. S.; Park, S. K.; Lee, I. K.; Kim, K. S.; Ahn, Y. H. SREBP-1c mediates the insulin-dependent hepatic glucokinase expression. *J. Biol. Chem.* **2004**, *279*, 30823–30829.

(25) Miyazaki, M.; Dobrzyn, A.; Man, W. C.; Chu, K.; Sampath, H.; Kim, H. J.; Ntambi, J. M. Stearoyl-CoA desaturase 1 gene expression is necessary for fructose-mediated induction of lipogenic gene expression by sterol regulatory element-binding protein-1c-dependent and -independent mechanisms. *J. Biol. Chem.* **2004**, *279*, 25164–25171.

(26) Horton, J. D.; Goldstein, J. L.; Brown, M. S. SREBPs: activators of the complete program of cholesterol and fatty acid synthesis in the liver. *J. Clin. Invest.* **2002**, *109*, 1125–1131.

(27) Awazawa, M.; Ueki, K.; Inabe, K.; Yamauchi, T.; Kaneko, K.; Okazaki, Y.; Bardeesy, N.; Ohnishi, S.; Nagai, R.; Kadowaki, T. Adiponectin suppresses hepatic SREBP1c expression in an AdipoR1/LKB1/AMPK dependent pathway. *Biochem. Biophys. Res. Commun.* **2009**, *382*, 51–56.

Supporting Information

RXR partial agonist CBt-PMN exerts therapeutic effects on type 2 diabetes without the side effects of RXR full agonists

Hiroki Kakuta,^{1*} Nobumasa Yakushiji,¹ Ryosuke Shinozaki,¹ Fuminori Ohsawa,¹ Shoya Yamada,¹ Yui Ohta,¹ Kohei Kawata,¹ Mariko Nakayama,¹ Manabu Hagaya,¹ Chisa Fujiwara,¹ Makoto Makishima,² Shigeyuki Uno,² Akihiro Tai,³ Ami Maehara,⁴ Masaru Nakayama,⁴ Toshitaka Oohashi,⁴ Hiroyuki Yasui,⁵ and Yutaka Yoshikawa⁵

1. Division of Pharmaceutical Sciences, Okayama University Graduate School of Medicine, Dentistry and Pharmaceutical Sciences, 1-1-1, Tsushima-Naka, Okayama 700-8530, Japan.

2. Division of Biochemistry, Department of Biomedical Sciences, Nihon University School of Medicine, 30-1 Oyaguchi-kamicho, Itabashi-ku, Tokyo 173-8610, Japan.

3. Faculty of Life and Environmental Sciences, Prefectural University of Hiroshima, 562 Nanatsuka-Cho, Shobara, Hiroshima 727-0023, Japan.

4. Division of Medical Sciences, Okayama University Graduate School of Medicine, Dentistry and Pharmaceutical Sciences, 2-5-1 Shikata-Cho, Kita-Ku, Okayama 700-8558, Japan.

5. Kyoto Pharmaceutical University, 5 Nakauchi-cho, Misasagi, Yamashina-ku, Kyoto 607-8414, Japan.

E-mail: kakuta@pharm.okayama-u.ac.jp

Contents:

1. Chemistry	S3–13
1.1. General	
1.2. Purity determination of compounds by HPLC	
1.3. Schemes	
Scheme S1	
Scheme S2	
1.4. Compound data	

2. Purity	S14
2.1. Combustion analysis data	
2.2. HPLC charts	
3. Luciferase Reporter Gene Assay	S15–17
3.1. Culture of COS-1 cells	
3.2. Luciferase reporter gene assay	
3.3. Supplementary data 1	
Figure S1. Dose-dependence of RXR α -agonistic activities of CBt-PMN (11b) and RXR α -antagonistic activity of CBt-PMN (11b) in the presence of 1 μ M LGD1069 (1).	
Figure S2. Relative transactivation activities toward RAR α , RAR β and RAR γ by NEt-TMN (5), CBiM-PMN (11a), and CBt-PMN (11b).	
Figure S3. Relative transactivation activities toward PPAR γ , PPAR γ /RXR α , LXR α , and LXR α /RXR α by NEt-TMN (5), CBiM-PMN (11a), and CBt-PMN (11b).	
4. In vivo assay	S18–26
4.1. Measurement of serum concentration of test compounds after oral administration of 30 mg/kg to mice.	
4.2. HPLC conditions	
4.3. Observation of side effects after once-daily oral administration of 30 mg/kg for 7 consecutive days in male ICR mice	
4.4. Observation of side effects after once-daily oral administration of 30 mg/kg for 28 consecutive days in SD rats	
4.5. Evaluation of blood glucose-lowering activity in KK-A ^y mice	
4.6. Measurements of blood parameters	
4.7. Measurements of metabolic parameters	
4.8. RNA Preparation and quantitative real-time RT-PCR	
4.9. Supplementary data 2	
Figure S4. Plasma concentrations of NEt-TMN (5), CBiM-PMN (11a) and CBt-PMN (11b) in ICR mice after single oral administration of 30 mg/kg.	
Figure S5. Evaluation of adverse effects of repeated oral administration of compounds at 30 mg/kg/day to male ICR mice for 7 consecutive days (n = 7–23).	

Figure S6. Body weight gain, water intake change, and food intake change of male or female SD rats treated with oral administration of vehicle or CBt-PMN (**11b**) at 30 mg/kg/day for 28 consecutive days

Table S2. Serum parameters of male ICR mice after oral administration of vehicle or CBt-PMN (**11b**) at 30 mg/kg/day for 7 consecutive days

Table S3. Organ weights of male or female SD rats after oral administration of vehicle or CBt-PMN (**11b**) at 30 mg/kg/day for 28 consecutive days

Table S4. Hematological and serum parameters of male and female SD rats after oral administration of vehicle or CBt-PMN (**11b**) at 30 mg/kg/day for 28 consecutive days

Table S5. Primer list

5. References

S27

1. Chemistry

1.1. General

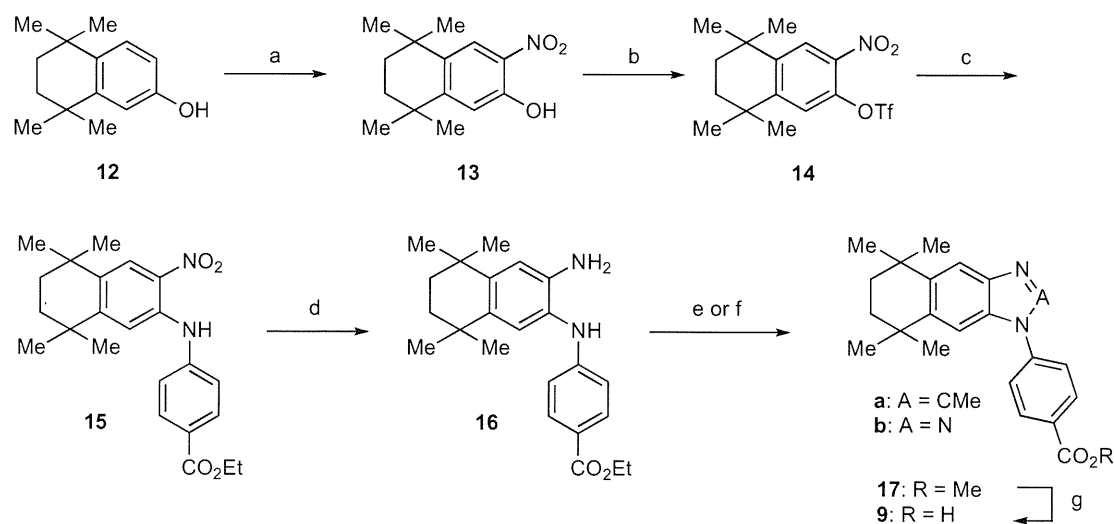
Melting points were determined with a Yanagimoto hot-stage melting point apparatus and are uncorrected. IR spectra were recorded on a JASCO FT/IR350 (KBr). ¹H-NMR spectra were recorded on a JEOL JNM-AL300 FT-NMR system (300 MHz) spectrometer, a VarianVXR-300 (300 MHz) or a VarianVXR-500 (500 MHz) spectrometer. Elemental analysis was carried out with a Yanagimoto MT-5 CHN recorder elemental analyzer and results were within ± 0.4% of the theoretical values. FAB-MS was carried out with a VG70-SE.

1.2. Purity determination of compounds by HPLC

Purity of compounds was determined by means of HPLC with a Shimadzu liquid chromatographic system (Kyoto, Japan) consisting of a LC-10AD pump, SPD-10AV UV-Vis spectrophotometric detector, CTO-10AS column oven and C-R5A Chromatopac. The chromatographic analyses were carried out on an Inertsil ODS-3 column (4.6 i.d. x 250 mm, 5 μm, GL Sciences, Tokyo, Japan) with a guard column of Inertsil ODS-3 (4.6 i.d. x 10 mm, 5 μm, GL Sciences) kept at 40°C, using methanol : 25 mM ammonium acetate (adjusted with acetic acid to pH 5.0) (80:20 v/v) as the mobile phase. The flow rate was 0.7 mL/min and the absorbance at 280 nm was monitored.

1.3. Schemes

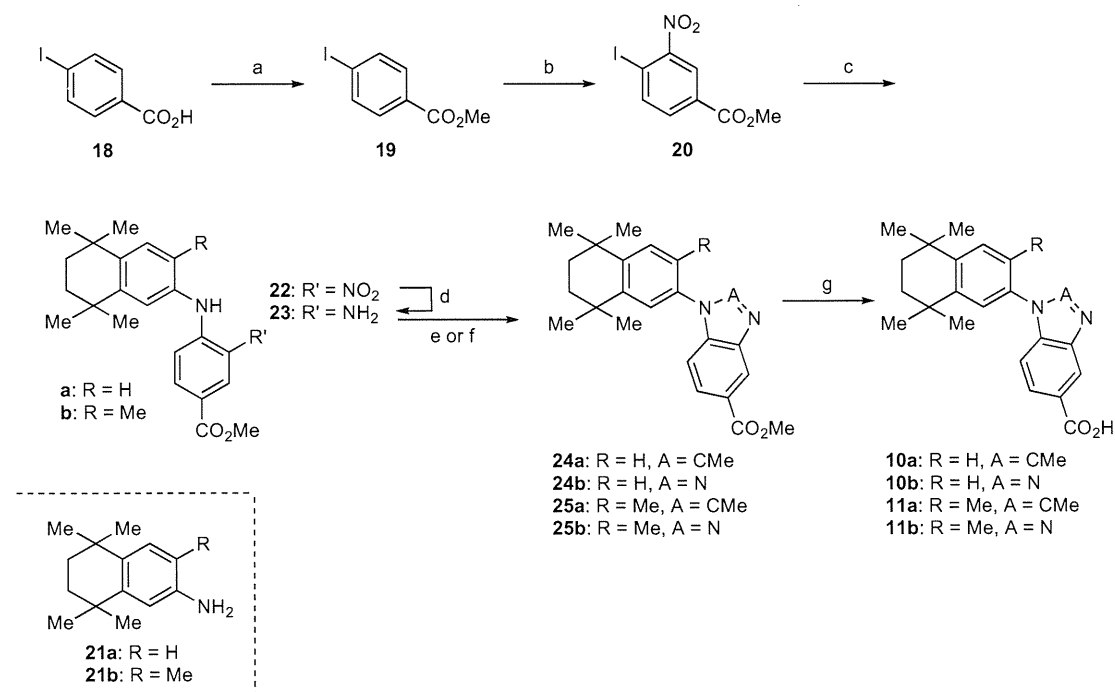
Scheme S1.^a



^a**Reagents and conditions:** a) *conc.* HNO₃, CH₂Cl₂, 0°C-rt. b) Tf₂O, pyridine, 0°C to rt. c) Ethyl 4-aminobenzoate, Pd₂(dba)₃, (±)-BINAP, Cs₂CO₃, dioxane, 100°C. d) H₂, Pd/C, EtOAc, EtOH, rt. e)

1) Ac₂O, AcOH, rt. 2) *p*-TsOH-H₂O, pyridine, dioxane, 110°C. f) NaNO₂, *conc.* H₂SO₄, THF, H₂O, 0°C to rt. g) 1) NaOH, MeOH, 60°C. 2) HCl.

Scheme S2.^a



“Reagents and conditions: a) MeOH, SOCl₂, 0-70°C. b) *conc.* HNO₃, *conc.* H₂SO₄, 0°C to rt. c) **21a** or **21b**, Pd₂(dba)₃, (±)-BINAP, Cs₂CO₃, toluene, 110°C. d) H₂, Pd/C, EtOAc, rt. e-1) 1) Ac₂O, AcOH, rt. 2) *p*-TsOH-H₂O, pyridine, dioxane, 120°C. e-2) 1) Ac₂O, AcOH, rt. 2) *p*-TsOH-H₂O, dioxane, 120°C. f) NaNO₂, H₂SO₄, THF, H₂O, 0°C. g) 1) NaOH, MeOH, 60°C. 2) HCl.

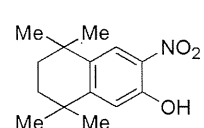
1.4. Compound data

4-[1-(3,5,5,8,8-Pentamethyl-5,6,7,8-tetrahydronaphthalen-2-yl)ethenyl]benzoic acid (**1**)

This compound was prepared according to reference S1.

6-[Ethyl(5,5,8,8-tetramethyl-5,6,7,8-tetrahydronaphthalen-2-yl)amino]nicotinic acid (**5**)

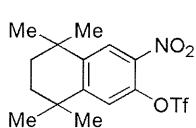
This compound was prepared according to reference S2.



5,5,8,8-Tetramethyl-3-nitro-5,6,7,8-tetrahydronaphthalen-2-ol (**13**).

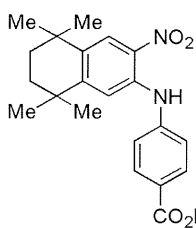
To an ice-cooled solution of **12** (2.0 g, 9.8 mmol) in CH₂Cl₂ (22 mL) was added *conc.* HNO₃ (0.75 mL) at 0°C. The mixture was stirred at r.t. under an Ar

atmosphere for 30 min, then poured onto ice and extracted with EtOAc (50 mL × 2). The organic layer was washed with H₂O (50 mL × 2) and brine (50 mL), dried over MgSO₄, filtered and evaporated under reduced pressure. The residue was recrystallized from MeOH to yield **13** as a pale yellow powder (640 mg, 26%). ¹H-NMR (300 MHz, CDCl₃) : δ 10.28 (s, 1H), 8.02 (s, 1H), 7.05 (s, 1H), 1.69 (s, 4H), 1.29 (s, 12H).



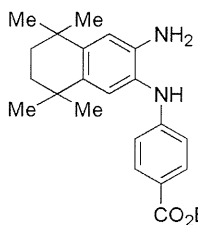
Trifluoromethanesulfonic acid 5,5,8,8-tetramethyl-3-nitro-5,6,7,8-tetrahydronaphthalen-2-yl ester (**14**).

To a solution of **13** (330 mg, 1.3 mmol) in dry pyridine (2.6 mL) was added trifluoromethanesulfonic anhydride (240 mL, 1.5 mmol) at 0°C. The mixture was stirred at r.t. under an Ar atmosphere for 9.0 hr, then poured into 2 mol/L HCl (30 mL) and extracted with EtOAc (50 mL × 3). The organic layer was washed with H₂O (30 mL × 2) and brine (20 mL), dried over MgSO₄, filtered and evaporated under reduced pressure. The residue was purified by flash column chromatography (EtOAc : *n*-hexane = 1 : 40) to yield **14** as a yellow powder (470 mg, 94%). ¹H-NMR (500 MHz, CDCl₃) : δ 8.10 (s, 1H), 7.27 (s, 1H), 1.73 (s, 4H), 1.33 (s, 6H), 1.30 (s, 6H).



4-(5,5,8,8-Tetramethyl-3-nitro-5,6,7,8-tetrahydronaphthalen-2-ylamino)-benzoic acid ethyl ester (**15**).

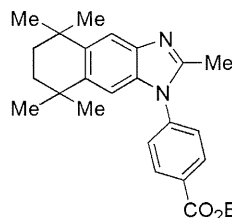
To a solution of **14** (740 mg, 1.9 mmol) and ethyl *p*-aminobenzoate (480 mg, 2.9 mmol) in dry dioxane (20 mL) were added Pd₂(dba)₃ (88 mg, 0.097 mmol), (±)-BINAP (90 mg, 0.14 mmol) and Cs₂CO₃ (940 mg, 2.9 mmol). The mixture was refluxed at 100°C for 30 min and filtered through Celite. The filtrate was evaporated under reduced pressure. The residue was purified by flash column chromatography (EtOAc : *n*-hexane = 1 : 60) to yield **15** as a red powder (600 mg, 78%). ¹H-NMR (300 MHz, CDCl₃) : δ 9.19 (s, 1H), 8.14 (s, 1H), 8.05 (d, *J* = 9.0 Hz, 2H), 7.43 (s, 1H), 7.25 (d, *J* = 9.0 Hz, 2H), 4.38 (q, *J* = 7.0 Hz, 2H), 1.70 (s, 4H), 1.40 (t, *J* = 7.0 Hz, 3H), 1.31 (s, 6H), 1.23 (s, 6H).



4-(3-Amino-5,5,8,8-tetramethyl-5,6,7,8-tetrahydronaphthalen-2-ylamino)-benzoic acid ethyl ester (**16**).

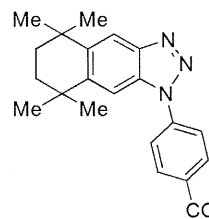
To a solution of **15** (200 mg, 0.50 mmol) in EtOAc (4.0 mL) and EtOH (1 mL) was added Pd/C (catalytic amount). The mixture was stirred at r.t. under an H₂ atmosphere overnight and filtered through Celite. The filtrate was evaporated under reduced pressure to yield **16** as a red oil (180 mg, 97%). ¹H-NMR (300 MHz, CDCl₃) : δ 7.87

(d, $J = 9.0$ Hz, 2H), 7.05 (s, 1H), 6.73 (s, 1H), 6.66 (d, $J = 9.0$ Hz, 2H), 5.68 (s, 1H), 4.31 (q, $J = 7.0$ Hz, 2H), 3.62 (br s, 2H), 1.65 (s, 4H), 1.35 (t, $J = 7.0$ Hz, 3H), 1.27 (s, 6H), 1.20 (s, 6H).



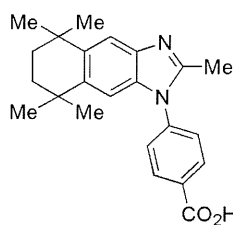
4-(2,5,5,8,8-Pentamethyl-5,6,7,8-tetrahydronaphtho[2,3-*d*]imidazol-1-yl)benzoic acid ethyl ester (**17a**).

To a solution of **16** (90 mg, 0.25 mmol) in AcOH (2.5 mL) was added Ac₂O (230 mL, 2.5 mmol). The mixture was stirred at r.t. for 40 min, poured into H₂O (20 mL) and extracted with EtOAc (40 mL × 2). The organic layer was washed with H₂O (20 mL) and brine (20 mL), dried over MgSO₄, filtered and evaporated under reduced pressure. The residue was purified by flash column chromatography (EtOAc : *n*-hexane = 1 : 5) to yield 4-(3-acetylamino-5,5,8,8-tetramethyl-5,6,7,8-tetrahydronaphthalen-2-ylamino)benzoic acid ethyl ester (90 mg). To a solution of this compound (90 mg, 0.22 mmol) in dioxane (2.2 mL) were added *p*-TsOH·H₂O (47 mg, 0.25 mmol) and dry pyridine (20 mL, 0.25 mmol). The mixture was refluxed at 110°C for 2.0 hr, poured into H₂O (30 mL) and extracted with EtOAc (30 mL × 2). The organic layer was washed with H₂O (30 mL) and brine (20 mL), dried over MgSO₄, filtered and evaporated under reduced pressure. The residue was purified by flash column chromatography (EtOAc : *n*-hexane = 1 : 10) to yield **17a** as a colorless powder (51 mg, 59%). ¹H-NMR (300 MHz, CDCl₃) : δ 8.28 (d, $J = 8.5$ Hz, 2H), 7.71 (s, 1H), 7.46 (d, $J = 8.5$ Hz, 2H), 7.07 (s, 1H), 4.45 (q, $J = 7.0$ Hz, 2H), 2.50 (s, 3H), 1.73 (s, 4H), 1.45 (t, $J = 7.0$ Hz, 3H), 1.37 (s, 6H), 1.26 (s, 6H).



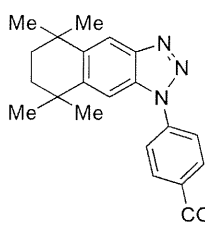
4-(5,5,8,8-Tetramethyl-5,6,7,8-tetrahydronaphtho[2,3-*d*][1,2,3]triazol-1-yl)benzoic acid ethyl ester (**17b**).

To an ice-cooled solution of **16** (86 mg, 0.24 mmol) in THF (6.3 mL) was added *conc.* H₂SO₄ (1.0 mL). Then, a solution of NaNO₂ (18 mg, 0.26 mmol) in H₂O (1.0 mL) was added dropwise. The mixture was stirred at r.t. for 1.5 hr, poured into 2 mol/L NaOH (10 mL) and extracted with EtOAc (30 mL × 2). The organic layer was washed with H₂O (40 mL) and brine (30 mL), dried over MgSO₄, filtered and evaporated under reduced pressure. The residue was purified by flash column chromatography (EtOAc : *n*-hexane = 1 : 20) to yield **17b** as an orange powder (87 mg, 98%). ¹H-NMR (300 MHz, CDCl₃) : δ 8.31 (d, $J = 9.0$ Hz, 2H), 8.12 (s, 1H), 7.90 (d, $J = 9.0$ Hz, 2H), 7.70 (s, 1H), 4.45 (q, $J = 7.0$ Hz, 2H), 1.79 (s, 4H), 1.45 (t, $J = 7.0$ Hz, 3H), 1.41 (s, 6H), 1.39 (s, 6H).



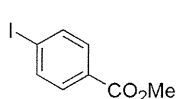
4-(2,5,5,8,8-Pentamethyl-5,6,7,8-tetrahydronaphtho[2,3-*d*]imidazol-1-yl)benzoic acid (**9a**).

To a solution of **17a** (51 mg, 0.13 mmol) in MeOH (1.3 mL) was added 2 mol/L NaOH (1.0 mL). The mixture was stirred at 60°C for 40 min, poured into 2 mol/L HCl (3 mL) and extracted with EtOAc (30 mL × 3). The organic layer was washed with H₂O (30 mL) and brine (20 mL), dried over MgSO₄, filtered and evaporated under reduced pressure to yield **9a** as a colorless solid (41 mg, 88%). The residue was recrystallized from MeOH to yield **9a** as a colorless powder (6.9 mg). Mp: 290.0-293.0°C; HPLC: 13.03 min. 96.6% purity; FAB-MS *m/z*: 363 [M+H]⁺. ¹H-NMR (500 MHz, DMSO-*d*₆) : δ 8.26 (d, *J* = 8.5 Hz, 2H), 7.82 (s, 1H), 7.78 (d, *J* = 8.5 Hz, 2H), 7.26 (s, 1H), 2.51 (s, 3H), 1.70 (s, 4H), 1.36 (s, 6H), 1.23 (s, 6H).



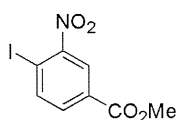
4-(5,5,8,8-Tetramethyl-5,6,7,8-tetrahydronaphtho[2,3-*d*][1,2,3]triazol-1-yl)benzoic acid (**9b**).

To a solution of **17b** (87 mg, 0.23 mmol) in MeOH (2.0 mL) was added 2 mol/L NaOH (1.0 mL). The mixture was stirred at 60°C for 2.5 hr, poured into 2 mol/L HCl (3 mL) and extracted with EtOAc (40 mL × 2). The organic layer was washed with H₂O (30 mL) and brine (20 mL), dried over MgSO₄, filtered and evaporated under reduced pressure to yield **9b** as a colorless solid (80 mg, q.y.). The residue was recrystallized from MeOH to yield **9b** as orange needles (33 mg, 41%). Mp: 275.0-279.0°C; HPLC: 13.50 min. 98.4% purity; ; FAB-MS *m/z*: 350 [M+H]⁺. ¹H-NMR (500 MHz, DMSO-*d*₆) : δ 13.2 (br s, 1H), 8.23 (d, *J* = 8.5 Hz, 2H), 8.18 (s, 1H), 8.03 (d, *J* = 8.5 Hz, 2H), 7.88 (s, 1H), 1.74 (s, 4H), 1.38 (s, 12H).



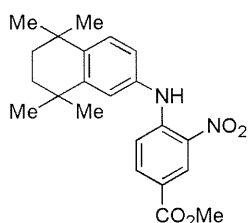
4-Iodobenzoic acid methyl ester (**19**).

To an ice-cooled solution of 4-iodobenzoic acid (5.0 g, 20 mmol) in MeOH (30 mL) was added SOCl₂ (2.6 mL, 30 mmol). The mixture was refluxed at 70°C for 1.0 hr, then evaporated with toluene to remove excess SOCl₂. The residue was dissolved in EtOAc (150 mL). The solution was washed with *sat.* NaHCO₃ (100 mL × 2) and brine (60 mL), dried over MgSO₄, filtered and evaporated under reduced pressure. The residue was recrystallized from CH₂Cl₂/*n*-hexane to yield **19** as colorless needles (4.7 g, 91%). ¹H-NMR (500 MHz, CDCl₃) : δ 7.80 (d, *J* = 8.0 Hz, 2H), 7.74 (d, *J* = 8.0 Hz, 2H), 3.91 (s, 3H).



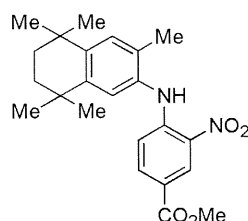
4-Iodo-3-nitrobenzoic acid methyl ester (**20**).

To an ice-cooled solution of **19** (1.3 g, 5.0 mmol) in *conc.* H₂SO₄ (5.0 mL) was added dropwise a solution of *conc.* HNO₃ (6.0 mL) and *conc.* H₂SO₄ (9.0 mL). The mixture was stirred at r.t. for 5.0 hr, then poured onto ice (100 mL), and extracted with EtOAc (60 mL × 2). The organic layer was washed with *sat.* NaHCO₃ (50 mL × 2) and brine (50 mL), dried over MgSO₄, filtered and evaporated under reduced pressure. The residue was recrystallized from CH₂Cl₂/*n*-hexane to yield **20** as yellow needles (1.2 g, 76%). ¹H-NMR (500 MHz, CDCl₃): δ 8.45 (d, *J* = 2.0 Hz, 1H), 8.15 (d, *J* = 8.0 Hz, 1H), 7.88 (dd, *J* = 8.0, 2.0 Hz, 1H), 3.97 (s, 3H).



3-Nitro-4-[*N*-(5,5,8,8-tetramethyl-5,6,7,8-tetrahydro-2-naphthyl)amino]benzoic acid methyl ester (**22a**).

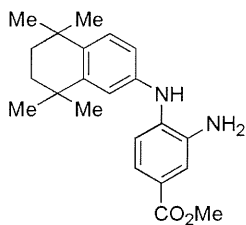
To a solution of **20** (1.1 g, 3.5 mmol) and **21a** (0.70 g, 3.5 mmol) in dry toluene (21 mL) were added Pd₂(dba)₃ (160 mg, 0.17 mmol), (±)-BINAP (160 mg, 0.26 mmol) and Cs₂CO₃ (1.6 g, 4.9 mmol). The mixture was refluxed at 110°C under an Ar atmosphere for 5.0 hr, then filtered through Celite. The filtrate was washed with H₂O (40 mL × 2) and brine (30 mL), dried over MgSO₄, filtered and evaporated under reduced pressure. The residue was purified by flash column chromatography (EtOAc : *n*-hexane = 1 : 5) and crystallized from *n*-hexane to yield **22a** as red needles (1.2 g, 76%). ¹H-NMR (500MHz, CDCl₃): δ 9.77 (br s, 1H), 8.91 (d, *J* = 2.0 Hz, 1H), 7.94 (dd, *J* = 9.0, 2.0 Hz, 1H), 7.37 (d, *J* = 8.0 Hz, 1H), 7.18 (d, *J* = 2.0 Hz, 1H), 7.16 (d, *J* = 9.0 Hz, 1H), 7.04 (dd, *J* = 8.0, 2.0 Hz, 1H), 3.91 (s, 3H), 1.72 (s, 4H), 1.31 (s, 6H), 1.28 (s, 6H).



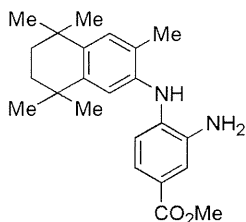
3-Nitro-4-[*N*-(3,5,5,8,8-pentamethyl-5,6,7,8-tetrahydro-2-naphthyl)amino]benzoic acid methyl ester (**22b**).

To a solution of **20** (0.92 g, 3.0 mmol) and **21b** (0.65 g, 3.0 mmol) in dry toluene (30 mL) were added Pd₂(dba)₃ (140 mg, 0.15 mmol), (±)-BINAP (140 mg, 0.22 mmol) and Cs₂CO₃ (1.4 g, 4.2 mmol). The mixture was refluxed at 110°C under an Ar atmosphere overnight, then filtered through Celite. The filtrate was evaporated under reduced pressure. The residue was purified by flash column chromatography (EtOAc : *n*-hexane = 1 : 10) to yield **22b** as a red foam (1.1 g, 94%). ¹H-NMR (300 MHz, CDCl₃): δ 9.63 (br s, 1H), 8.93 (d, *J* = 2.0 Hz, 1H), 7.93 (dd, *J* = 9.0, 2.0 Hz, 1H), 7.24 (s, 1H), 7.17 (s, 1H), 6.82 (d, *J* = 9.0 Hz, 1H), 3.91 (s, 3H), 2.19 (s, 3H), 1.70 (s, 4H), 1.31 (s, 6H), 1.25 (s, 6H).

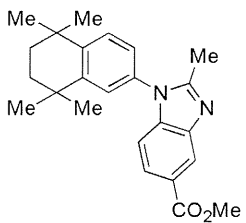
3-Amino-4-[*N*-(5,5,8,8-tetramethyl-5,6,7,8-tetrahydro-2-naphthylamino)benzoic acid methyl ester (**23a**).



To a solution of **22a** (760 mg, 2.0 mmol) in EtOAc (10 mL) was added Pd/C (catalytic amount). The mixture was stirred at r.t. under an H₂ atmosphere overnight, then filtered through Celite. The filtrate was evaporated under reduced pressure. The residue was recrystallized from CH₂Cl₂/*n*-hexane to yield **23a** as colorless needles (660 mg, 94%). ¹H-NMR (500 MHz, CDCl₃) : δ 7.48 (s, 1H), 7.48 (d, *J* = 9.0 Hz, 1H), 7.23 (d, *J* = 8.5 Hz, 1H), 7.14 (d, *J* = 9.0 Hz, 1H), 6.94 (s, 1H), 6.81 (d, *J* = 8.5 Hz, 1H), 5.52 (s, 1H), 3.87 (s, 3H), 3.57 (br s, 2H), 1.69 (s, 4H), 1.28 (s, 6H), 1.26 (s, 6H).

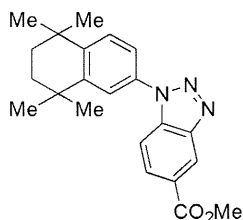


3-Amino-4-[*N*-(3,5,5,8,8-pentamethyl-5,6,7,8-tetrahydro-2-naphthyl)amino]benzoic acid methyl ester (**23b**). To a solution of **22b** (1.1 g, 2.8 mmol) in EtOAc (20 mL) was added Pd/C (catalytic amount). The mixture was stirred at r.t. under an H₂ atmosphere for 1.0 hr, then filtered through Celite. The filtrate was evaporated under reduced pressure to yield **23b** as a white solid (1.0 g, 97%). ¹H-NMR (300 MHz, CDCl₃) : δ 7.49 (s, 1H), 7.48 (d, *J* = 8.0 Hz, 1H), 7.13 (s, 1H), 6.96 (s, 1H), 6.83 (d, *J* = 8.0 Hz, 1H), 5.39 (br s, 1H), 3.87 (s, 3H), 3.55 (br s, 2H), 2.19 (s, 3H), 1.67 (s, 4H), 1.28 (s, 6H), 1.21 (s, 6H).

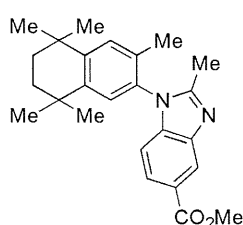


2-Methyl-1-[(5,5,8,8-tetramethyl-5,6,7,8-tetrahydronaphthalen-2-yl)-1H-benzimidazole-5-carboxylic acid methyl ester (**24a**). To a solution of **23a** (180 mg, 0.50 mmol) in AcOH (5.0 mL) was added Ac₂O (0.50 mL). The mixture was stirred at r.t. for 20 min, then poured into ice-cooled 2 mol/L NaOH (50 mL) and extracted with EtOAc (30 mL × 2). The organic layer was washed with H₂O (40 mL × 2) and brine (30 mL), dried over MgSO₄, filtered and evaporated under reduced pressure. The residue was recrystallized from CH₂Cl₂/*n*-hexane to yield colorless needles (180 mg). To a solution of the residue (160 mg) in dioxane were added *p*-TsOH·H₂O (76 mg, 0.40 mmol) and pyridine (32 mL, 0.40 mmol). The solution was refluxed at 120°C for 5.0 hr, then poured into H₂O (80 mL) and extracted with EtOAc (30 mL × 2). The organic layer was washed with H₂O (40 mL × 2) and brine (30 mL), dried over MgSO₄, filtered and evaporated under reduced pressure. The residue was re-crystallized from CH₂Cl₂/*n*-hexane to yield **24a** as colorless needles (110 mg, 65%). ¹H-NMR (500 MHz, CDCl₃) : δ 8.44 (s, 1H), 7.93 (d, *J* = 8.0 Hz, 1H), 7.48 (d, *J* = 8.0 Hz, 1H), 7.26 (s, 1H), 7.17 (d, *J* = 8.0 Hz, 1H), 7.10 (d, *J* = 8.0 Hz, 1H), 3.95 (s, 3H), 2.54 (s, 3H), 1.76 (s, 4H), 1.36 (s, 6H), 1.31 (s, 6H).

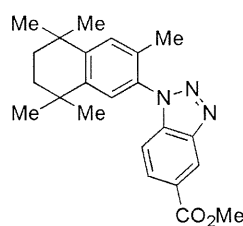
1-[(5,5,8,8-Tetramethyl-5,6,7,8-tetrahydro-2-naphthyl)-1H-benzotriazole-5-carboxylic acid methyl ester (**24b**).



To an ice-cooled solution of **23a** (180 mg, 0.5 mmol) in THF (3.0 mL) was added a mixture of *conc.* H₂SO₄ (1.0 mL) and H₂O (10 mL). Then, a solution of NaNO₂ (48 mg, 0.7 mmol) in H₂O (1.0 mL) was added dropwise. The mixture was stirred at 0°C for 20 min, poured into H₂O (30 mL) and extracted with EtOAc (30 mL × 2). The organic layer was washed with H₂O (40 mL) and brine (30 mL), dried over MgSO₄, filtered and evaporated under reduced pressure. The residue was purified by flash column chromatography (EtOAc : *n*-hexane = 1 : 3) to yield **24b** as an orange solid (180 mg, 99 %). ¹H-NMR (500 MHz, CDCl₃) : δ 8.87 (s, 1H), 8.23 (d, *J* = 9.0 Hz, 1H), 7.73 (d, *J* = 8.0 Hz, 1H), 7.66 (d, *J* = 2.0 Hz, 1H), 7.55 (d, *J* = 9.0 Hz, 1H), 7.49 (d, *J* = 8.0, 2.0 Hz, 1H), 4.00 (s, 3H), 1.77 (s, 4H), 1.36 (s, 12H).

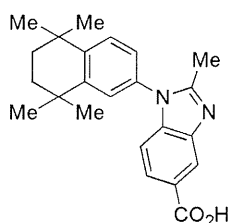


2-Methyl-1-(3,5,5,8,8-pentamethyl-5,6,7,8-tetrahydro-2-naphthyl)-1H-benzimidazole-5-carboxylic acid methyl ester (**25a**). To a solution of **23b** (150 mg, 0.4 mmol) in AcOH (5.0 mL) was added Ac₂O (0.5 mL). The mixture was stirred at r.t. for 15 min, then poured into ice-cooled *sat.* NaHCO₃ (70 mL) and extracted with EtOAc (50 mL × 2). The organic layer was washed with *sat.* NaHCO₃ (70 mL), dried over MgSO₄, filtered and evaporated under reduced pressure. The residue (170 mg) and *p*-TsOH·H₂O (190 mg, 1.0 mmol) were dissolved in dioxane (5.0 mL). The solution was refluxed at 120°C overnight, then poured into H₂O (40 mL) and extracted with EtOAc (30 mL × 2). The organic layer was washed with H₂O (50 mL) and brine (30 mL), dried over MgSO₄, filtered and evaporated under reduced pressure to yield **25a** as a brown solid (150 mg, 98%). ¹H-NMR (500 MHz, CDCl₃) : δ 8.46 (d, *J* = 1.5 Hz, 1H), 7.92 (dd, *J* = 8.5, 1.5 Hz, 1H), 7.30 (s, Ar-H, 1H), 7.12 (s, 1H), 6.98 (s, 1H), 3.95 (s, 3H), 2.42 (s, 3H), 1.90 (s, 3H), 1.74 (s, 4H), 1.36 (s, 6H), 1.26 (s, 6H).



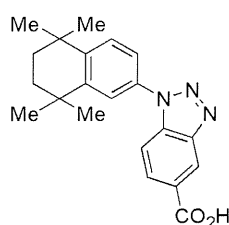
1-(3,5,5,8,8-Pentamethyl-5,6,7,8-tetrahydro-2-naphthyl)-1H-benzotriazole-5-carboxylic acid methyl ester (**25b**). To an ice-cooled solution of **23b** (150 mg, 0.40 mmol) in THF (2.0 mL) was added a mixture of *conc.* H₂SO₄ (1.0 mL) and H₂O (10 mL). Then, a solution of NaNO₂ (41 mg, 0.60 mmol) in H₂O (2.0 mL) was added dropwise. The reaction mixture was refluxed at 0°C for 30 min, poured into H₂O (20 mL), and extracted with EtOAc (30 mL × 2). The organic layer was washed with H₂O (40 mL) and brine (30 mL), dried over MgSO₄, filtered and evaporated under reduced pressure. The residue was purified by flash column chromatography (EtOAc : *n*-hexane = 1 : 1). The product was again purified by flash column chromatography (EtOAc : *n*-hexane = 1 : 3) to yield **25b** as an orange solid (140 mg, 91 %). ¹H-NMR (500 MHz, CDCl₃) : δ 8.87 (d, *J* = 1.5 Hz, 1H), 8.19 (dd, *J* = 8.5, 1.5 Hz,

1H), 7.40 (d, $J = 8.5$ Hz, 1H), 7.35 (s, 1H), 7.29 (s, 1H), 4.00 (s, 3H), 2.07 (s, 3H), 1.75 (s, 4H), 1.36 (s, 6H), 1.29 (s, 6H).



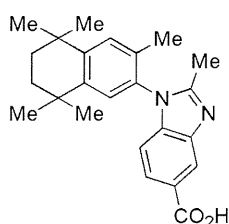
2-Methyl-1-(5,5,8,8-tetramethyl-5,6,7,8-tetrahydro-2-naphthyl)-1H-benzimidazole-5-carboxylic acid (**10a**).

To a solution of **24a** (87 mg, 0.23 mmol) in MeOH (10 mL) was added 2 mol/L NaOH (10 mL). The mixture was stirred at 60°C for 20 min, poured into 1 mol/L HCl (20 mL) and extracted with EtOAc (30 mL \times 3). The organic layer was washed with H₂O (60 mL) and brine (40 mL), dried over MgSO₄, filtered and evaporated under reduced pressure to yield **10a** as a white solid (65 mg, 78%). Mp > 295°C; ¹H-NMR (500 MHz, DMSO-*d*₆) : δ 12.71 (br s, 1H), 8.19 (s, 1H), 7.82 (d $J = 8.5$ Hz, 1H), 7.58 (d, $J = 8.5$ Hz, 1H), 7.51 (s, 1H), 7.29 (d, $J = 8.0$ Hz, 1H), 7.19 (d, $J = 8.0$ Hz, 1H), 2.47 (s, 3H), 1.71 (s, 4H), 1.33 (s, 6H), 1.29 (s, 6H); IR (KBr) : $\nu = 2960$ (OH), 1698 (CO) cm⁻¹; FAB-MS m/z : 363 [M+H]⁺.



1-(5,5,8,8-Tetramethyl-5,6,7,8-tetrahydro-2-naphthyl)-1H-benzotriazole-5-carboxylic acid (**10b**).

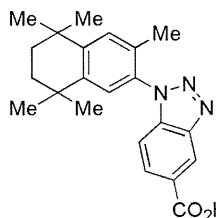
To a solution of **24b** (180 mg, 0.5 mmol) in MeOH (10 mL) was added 2 mol/L NaOH (8.0 mL). The mixture was stirred at 60°C for 15 min, poured into 1 mol/L HCl (20 mL), and extracted with EtOAc (30 mL \times 2). The organic layer was washed with H₂O (40 mL \times 2) and brine (30 mL), dried over MgSO₄, filtered and evaporated under reduced pressure to yield **10b** as an orange solid (170 mg, q.y.). Mp: 260.0-261.0°C; ¹H-NMR (300 MHz, DMSO-*d*₆) : δ 13.39 (br s, 1H), 8.72 (d, $J = 1.5$ Hz, 1H), 8.19 (d, $J = 9.0$, 1.5 Hz, 1H), 7.90 (d, $J = 9.0$ Hz, 1H), 7.77 (d, $J = 2.0$ Hz, 1H), 7.67 (d, $J = 8.5$ Hz, 1H), 7.60 (d, $J = 8.5$, 2.0 Hz, 1H), 1.73 (s, 4H), 1.34 (s, 12H); IR (KBr): $\nu = 2961$ -2933 (OH), 1713 (CO) cm⁻¹; FAB-MS m/z : 350 [M+H]⁺.



2-Methyl-1-(3,5,5,8,8-pentamethyl-5,6,7,8-tetrahydro-2-naphthyl)-1H-benzimidazole-5-carboxylic acid (**11a** : CBiM-PMN).

To a solution of **25a** (150 mg, 0.4 mmol) in MeOH (10 mL) was added 2 mol/L NaOH (10 mL). The mixture was stirred at 60°C for 20 min, poured into 1 mol/L HCl (20 mL) and extracted with EtOAc (30 mL \times 2). The organic layer was washed with H₂O (40 mL) and brine (30 mL), dried over MgSO₄, filtered and evaporated under reduced pressure to yield **11a** as a brown solid (140 mg, 93%). The residue was recrystallized from MeOH to yield a colorless powder (84 mg). Mp: 295.0°C; ¹H-NMR (300 MHz, DMSO-*d*₆) : δ 12.71 (br s, 1H), 8.20 (s, 1H), 7.81 (d $J = 8.5$ Hz, 1H), 7.47 (s, 1H), 7.36

(s, 1H), 6.94 (d, $J = 8.5$ Hz, 1H), 2.32 (s, 3H), 1.85 (s, 3H), 1.69 (s, 4H), 1.33 (s, 6H), 1.25 (s, 3H), 1.24 (s, 3H); IR (KBr): $\nu = 2957\text{-}2925$ (OH), 1701 (CO) cm^{-1} ; FAB-MS m/z : 377 $[\text{M}+\text{H}]^+$.



1-(3,5,5,8,8-Pentamethyl-5,6,7,8-tetrahydro-2-naphthyl)-1H-benzotriazole-5-carboxylic acid (**11b**: CBt-PMN).

To a solution of **25b** (140 mg, 0.36 mmol) in MeOH (6.0 mL) was added 2 mol/L NaOH (6.0 mL). The mixture was stirred at 60°C for 15 min, poured into 1 mol/L HCl (12 mL), and extracted with EtOAc (20 mL \times 2). The organic layer was washed with H₂O (20 mL) and brine (20 mL), dried over MgSO₄, filtered and evaporated under reduced pressure to yield **11b** as a pale yellow solid (120 mg, 86%). The residue was recrystallized from EtOAc/*n*-hexane as colorless needles. Mp: 238.0-239.0°C; ¹H-NMR (300 MHz, DMSO-*d*₆) : δ 13.26 (1H, br s), 8.72 (1H, d, $J = 1.5$ Hz), 8.14 (1H, dd, $J = 8.5, 1.5$ Hz), 7.56 (1H, d, $J = 8.5$ Hz), 7.52 (1H, s), 7.49 (1H, s), 2.00 (3H, s), 1.71 (4H, s), 1.34 (6H, s), 1.27 (6H, s); IR (KBr): $\nu = 2961$ (OH), 1714 (CO) cm^{-1} ; FAB-MS m/z : 364 $[\text{M}+\text{H}]^+$.

2. Purity

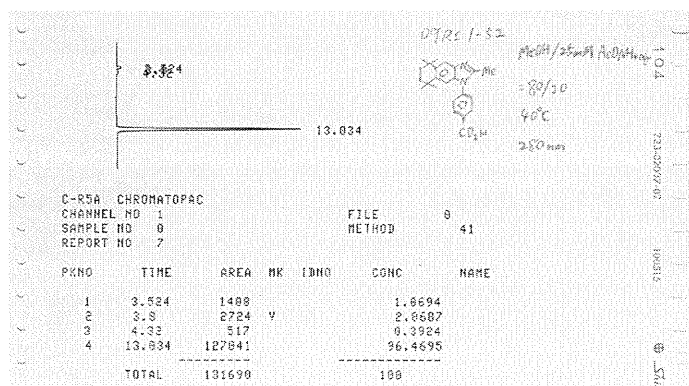
2.1. Combustion analysis data

Table S1. Combustion analysis data for compounds **10a**, **10b**, **11a**, and **11b**

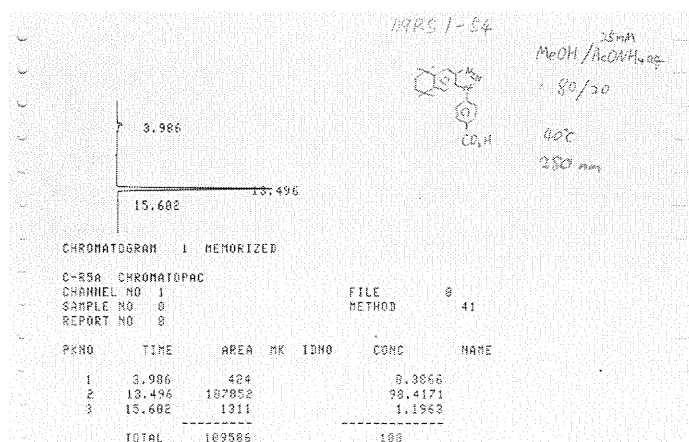
compound	Formula	Calculated			Found		
		C	H	N	C	H	N
10a	$C_{23}H_{26}N_2O_2 \cdot 5/3H_2O$	70.38	7.53	7.14	70.61	7.27	6.97
10b	$C_{21}H_{23}N_3O_2$	72.18	6.63	12.03	72.02	6.79	11.93
11a	$C_{24}H_{28}N_2O_2$	76.56	7.50	7.44	76.31	7.65	7.40
11b	$C_{22}H_{25}N_3O_2$	72.70	72.70	11.56	72.55	6.97	11.54

2.2. HPLC Charts

9a:



9b:



3. Luciferase Reporter Gene Assay

3.1. Culture of COS-1 cells

COS-1 cells were maintained in Dulbecco's modified Eagle's medium supplemented with 10% FBS in a humidified atmosphere of 5% CO₂ in air at 37°C.

3.2. Luciferase reporter gene assay

Luciferase reporter gene assays were performed using COS-1 cells transfected with three kinds of vectors: each receptor subtype, a luciferase reporter gene under the control of the appropriate RXR response element, and secreted alkaline phosphatase (SEAP) gene as a background. CRBP_{II}-tk-Luc, tk-PPRE₃-Luc, and tk-rBAR_{x3}-Luc reporters were used as RXR, PPAR, and LXR response elements, respectively. The amounts of each receptor subtype and response element were 1.0 µg and 4.0 µg, respectively. Transfection was performed with QIA Effectene Transfection reagent according to the supplier's protocol. In the case of heterodimer assay, RXR α (0.5 µg), each partner receptor (PPAR γ or LXR α , 0.5 mg) and the partner response element (4.0 µg) were transfected into COS-1 cells as described above. Test compound solutions (DMSO concentration below 1%) were added to the suspension of transfected cells, which were seeded at about 2.0×10⁴ cells/well in 96-well white plates. After incubation in a humidified atmosphere of 5% CO₂ at 37°C for 18 h, 25 µL of the medium was used for analyzing SEAP activities and the remaining cells were used for luciferase reporter gene assays with a Steady-Glo Luciferase Assay system (Promega) according to the supplier's protocol. The luciferase activities were normalized using SEAP activities. The assays were carried out in triplicate three times.

3.3 Supplementary data 1

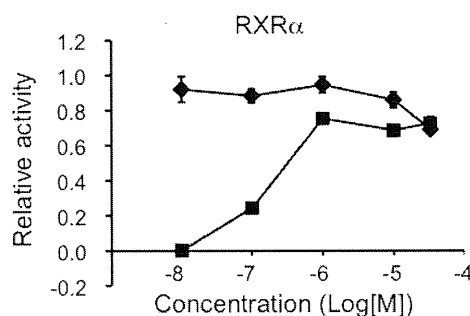


Figure S1. Dose-dependence of RXR α -agonistic activities of CBt-PMN (**11b**) (squares) and RXR α -antagonistic activity of CBt-PMN (**11b**) in the presence of 1 µM LGD1069 (**1**) (diamonds). The transactivation activity is shown as relative activity based on the luciferase activity of 1 µM LGD1069 (**1**) taken as 1.0. Error bars are s.e.m.

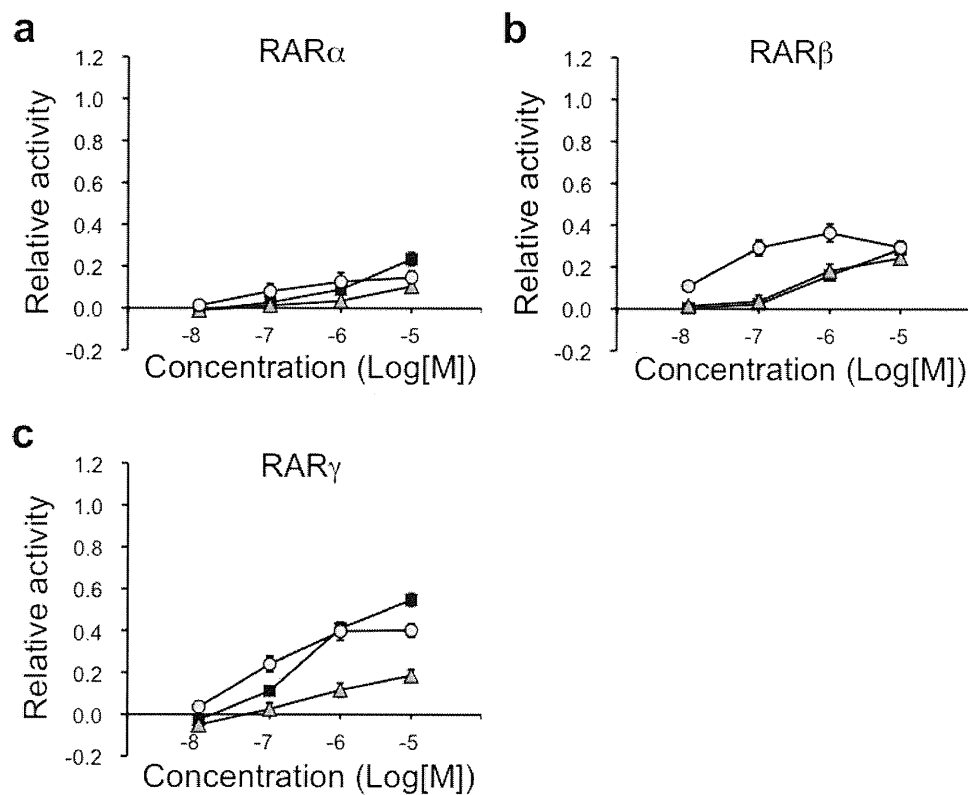


Figure S2. Relative transactivation activities toward RAR α , RAR β and RAR γ by NEt-TMN (**5**), CBiM-PMN (**11a**), and CBt-PMN (**11b**). The data are relative activity with respect to the luciferase activity of 1 μ M Am80 (RAR α / β selective agonist) (*S3*) (toward RAR α / β) or ATRA (toward RAR γ) taken as 1.0. Circles, triangles, and squares indicate NEt-TMN (**5**), CBiM-PMN (**11a**), and CBt-PMN (**11b**), respectively. The data ($n = 3$) represent the mean \pm s.e.m.

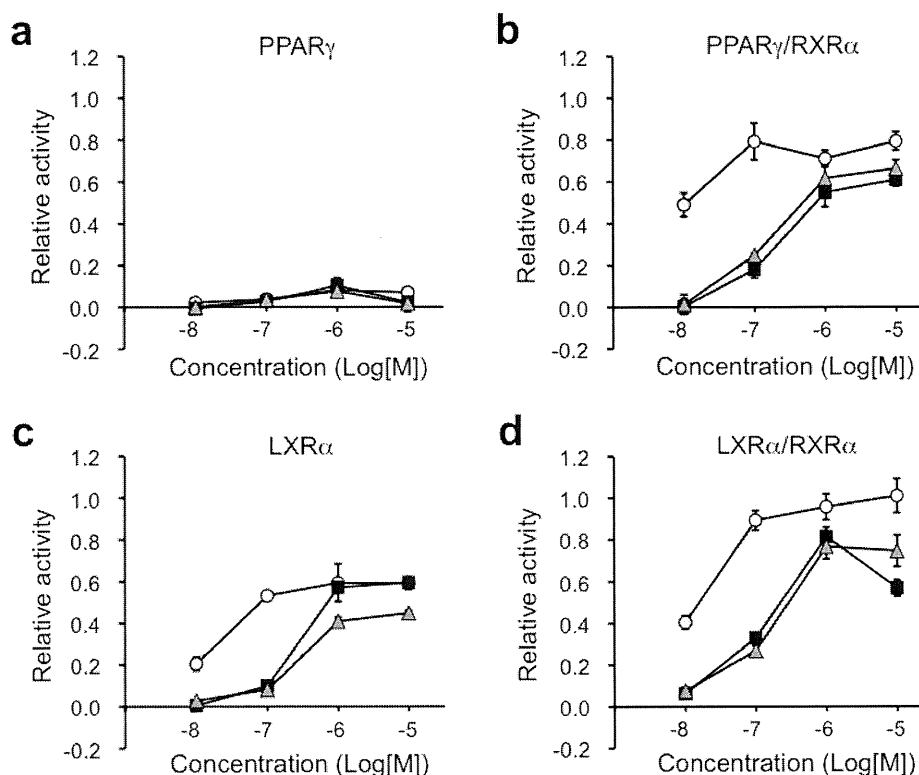


Figure S3. Relative transactivation activities toward PPAR γ , PPAR γ /RXR α , LXR α , and LXR α /RXR α by NEt-TMN (**5**), CBiM-PMN (**11a**), and CBt-PMN (**11b**). The data are relative activity with respect to the luciferase activity of 1 μ M LGD1069 (**1**) taken as 1.0. **(a)** Relative transactivation data for PPAR γ , based on the luciferase activity of 1 μ M TIPP703 (PPAR pan-agonist) taken as 1.0. **(b)** Relative transactivation data for PPAR γ /RXR α , based on the luciferase activity of 1 μ M TIPP703 taken as 1.0. **(c)** Relative transactivation data for LXR α , based on the luciferase activity of 1 μ M carba-T0901317 (LXR pan-agonist) taken as 1.0. **(d)** Relative transactivation data for LXR α /RXR α , based on the luciferase activity of 1 μ M carba-T0901317 taken as 1.0. TIPP703 or carba-T0901317 at 1 μ M give each E_{\max} value. Circles, triangles, and squares indicate NEt-TMN (**5**), CBiM-PMN (**11a**), and CBt-PMN (**11b**), respectively. The data ($n = 3-6$) represent the mean \pm s.e.m.

4. In vivo assay

4.1. Measurement of serum concentration of test compounds after oral administration of 30 mg/kg to mice

Groups of six-week-old ICR male mice (n = 5-9 in each) were treated with solutions of test compound 30 mg/kg (1% ethanol and 0.5% CMC in distilled water) at a volume of 10 mL/kg of body weight by oral administration. At the indicated times, 0.6 mL of blood was taken from the inferior vena cava under diethyl ether anesthesia. Each blood sample was centrifuged at 9,000 rpm for 5 min at r.t. To 100 μ L of the resulting plasma were added 100 μ L of ice-cold 5 mM ammonium acetate solution (adjusted with acetic acid to pH 5.0) and 1 mL of ice-cold ethyl acetate. The resulting mixture was vortexed for 30 sec, kept at room temperature for 10 min, and centrifuged at 9,000 rpm for 30 sec at room temperature. An 800 μ L aliquot of the ethyl acetate phase was removed and concentrated to dryness in a centrifugal evaporator. To the resulting residue was added 100 μ L of HPLC-grade methanol. This solution was directly subjected to HPLC analysis, and the concentration of each compound was determined from the peak area of the sample with reference to a calibration plot obtained with the authentic compound.

4.2. HPLC conditions

The HPLC system used in this study was a Shimadzu liquid chromatographic system (Kyoto, Japan) consisting of an SCL-10A system controller, LC-10AD pump, SPD-10AV UV-Vis spectrophotometric detector, SIL-10AD autoinjector, CTO-10A column oven, DGU-14A degasser and C-R7A Chromatopac. The samples (each 20 μ L) were injected using a refrigerated autosampler kept at 10°C. The chromatographic analyses were carried out on an Inertsil ODS-3 (4.6 i.d. x 250 mm, 5 mm, GL Sciences, Tokyo, Japan) kept at 40°C, using methanol : 33.3 mM ammonium acetate (adjusted with acetic acid to pH 5.0) (85:15, v/v) as a mobile phase. The flow rate was 0.7 mL/min and the absorbance at 280 nm was monitored.

4.3. Observation of side effects after once-daily oral administration of 30 mg/kg for 7 consecutive days in male ICR mice

Six-week-old male ICR mice were purchased from Charles River Laboratories Japan, Inc.. This experiment was conducted in accordance with the Guidelines for Animal Experiments at Okayama University Advanced Science Research Center, and all procedures were approved by the Animal Research Control Committee of Okayama University. After the arrival of the animals, all were group-housed and acclimated to the colony for 1 day before the experiment. Before the experiment, they were housed with four mice per cage, with free access to water and chow pellets in a light (12 hr on, 8:00 A.M. /12 hr off, 8:00 P.M.), temperature (23 \pm 1°C), and relative humidity (50 \pm 20%)-controlled environment. At 1 day before experiments, mice were assigned to experimental groups to minimize the variance between groups based on the measured weight (four per cage (17 x 33 x 15